Preliminary investigation of geological controls on radon concentration in surficial sediment in Whitehorse, Yukon (NTS 105D/11, 14)

Michael J. Kishchuk* and John C. Gosse
Department of Earth and Environmental Sciences, Dalhousie University

Panya S. Lipovsky and Jeffrey D. Bond
Yukon Geological Survey

Kishchuk, M.J., Lipovsky, P.S., Bond, J.D. and Gosse, J.C., 2021. Preliminary investigation of geological controls on radon concentration in surficial sediment in Whitehorse, Yukon (NTS 105D/11, 14). *In:* Yukon Exploration and Geology 2020, K.E. MacFarlane (ed.), Yukon Geological Survey, p. 115–135.

Abstract

Although the presence of radon has been reported in Yukon, the controls on radon soil gas fluxes in Yukon have not been studied. Here we report 328 radon concentration measurements collected in surficial sediment at 30 sites throughout Whitehorse during the summer of 2020 for the purpose of examining the controlling factors. The sediment types include till, glaciofluvial sand and gravel, glaciolacustrine silt, fluvial sand and gravel, and eolian sand. Average radon concentrations were compared to bedrock lithology, thickness of surficial sediment, surficial sediment type, surficial sediment grain size distribution, sorting, sediment maturity, and soil moisture to determine the first-order geological controls. Pronounced interseasonal variation was observed, but intraseasonal summer readings were relatively consistent. Positive correlation is apparent between radon concentration and grain size distribution, as well as between radon concentration and soil moisture. Negative correlation is observed between radon concentration and sediment maturity, with till and weathered bedrock displaying the highest concentrations of radon. No appreciable correlation was observed with depth to bedrock or with bedrock type. Additional data are being collected to complete the analyses in order to establish which geological and environmental factors are primary controls on radon concentration in near surface sediments.

* *mc723665@dal.ca*

Introduction

Radon is a colourless, odourless carcinogenic gas which occurs naturally in soil and rock, and which may enter homes via openings and cracks in foundations. While not dangerous in outdoor settings where it quickly dissipates, radon poses a major public health hazard when it accumulates in poorly ventilated basements. As of 2018, nearly 4400 Yukon homes have been tested for indoor radon, with more than 3300 measurements in the greater Whitehorse area (Yukon Housing Corporation, 2018). Of these, some 17 of 44 subdivisions (Fig. 1) have average indoor concentrations of radon gas higher than Health Canada's guideline of 200 Bq m^{-3} (Government of Canada, 2020). World Health Organization (WHO) guidelines are even lower, recommending mitigation if indoor radon concentration exceeds 100 Bq m^{-3}.

While many international studies accept that bedrock uranium concentration is the strongest control on radon concentration in urban regions (e.g., Stanley *et al*., 2019; Cinelli *et al*., 2015), attention must also be given to the overlying surficial sediment. This is particularly important in areas where sediment cover is thicker than the diffusion distance of radon over its radioactive lifetime (the half-life of ^{222}Rn is 3.8 days, (Marin, 1956)). In these areas, the physical and chemical properties of the surficial cover could potentially be significant controls on radon flux. Additionally, while uranium concentration in the Whitehorse suite of granitoid rocks is generally low (Yukon Geological Survey, 2020b), high indoor radon values have been measured, potentially indicating non-granitoid radon sources.

This study aims to compare the effect of several geological and meteorological controls on spatial and temporal variability in the flux of soil radon gas, with a long-term goal of understanding how to better predict and mitigate risks associated with radon. In Canada, radon is considered a carcinogen (Government of Canada, 2020) and, after inhalation, its pulmonary effect is compounded when the decay of gaseous ^{222}Rn produces heavy metals ^{210}Po, ^{214}Pb, ^{214}Bi and ^{214}Po. These heavy metals adhere to aerosols and accumulate in the lungs where in turn they produce alpha, beta and gamma radiation (Porstendorfer, 1994). Knowledge of radon source and distribution is necessary to inform public health policy, such as building codes and workplace conditions. By measuring radon in different representative undisturbed natural sediment types, and by documenting which factors have first-order control on soil radon flux variability, we can establish where and when radon exceeds concentration guidelines, and can more accurately predict radon concentration in untested regions of the territory.

The Yukon Geological Survey (YGS) is working to better understand the distribution of radon in surficial materials. The objective of this study is to determine if there is temporal or spatial variability of radon concentration at sites undisturbed by anthropogenic modification and if so, what factors control that variability. Our preliminary results reveal that temporal variation occurs seasonally, and that spatial variation is at least partly controlled by sediment grain-size distribution and maturity. Since the composition and thickness of surficial deposits throughout Yukon are non-uniform, these findings may warrant consideration in future building codes and health policies regarding radon gas.

Background

Geologic setting

Bedrock geology

Four major bedrock lithologic units underlie the Whitehorse area (Hart and Radloff, 1990; Colpron, 2011; and Yukon Geological Survey, 2020a): the limestone Hancock member and the clastic sedimentary Mandanna member of the Aksala formation; Whitehorse pluton granitic rocks; and the Miles Canyon Basalt (Fig. 2). The Hancock and Mandanna members of the Aksala formation were deposited during the upper Triassic in a coastal fluvial setting. The Hancock member is composed of massive and thickly bedded limestone with some dolostone, limestone debris flow conglomerate, and minor chert. The Mandanna member is composed of sandstone and polymictic conglomerate, along with mudstone and minor bioturbated sandstone. The Whitehorse batholith intruded these Triassic units in the mid-Cretaceous, between 112 and 105 Ma. In the study area, these rocks are characterized as medium to coarse-grained granodiorite and diorite. Uranium concentration in the Whitehorse suite varies

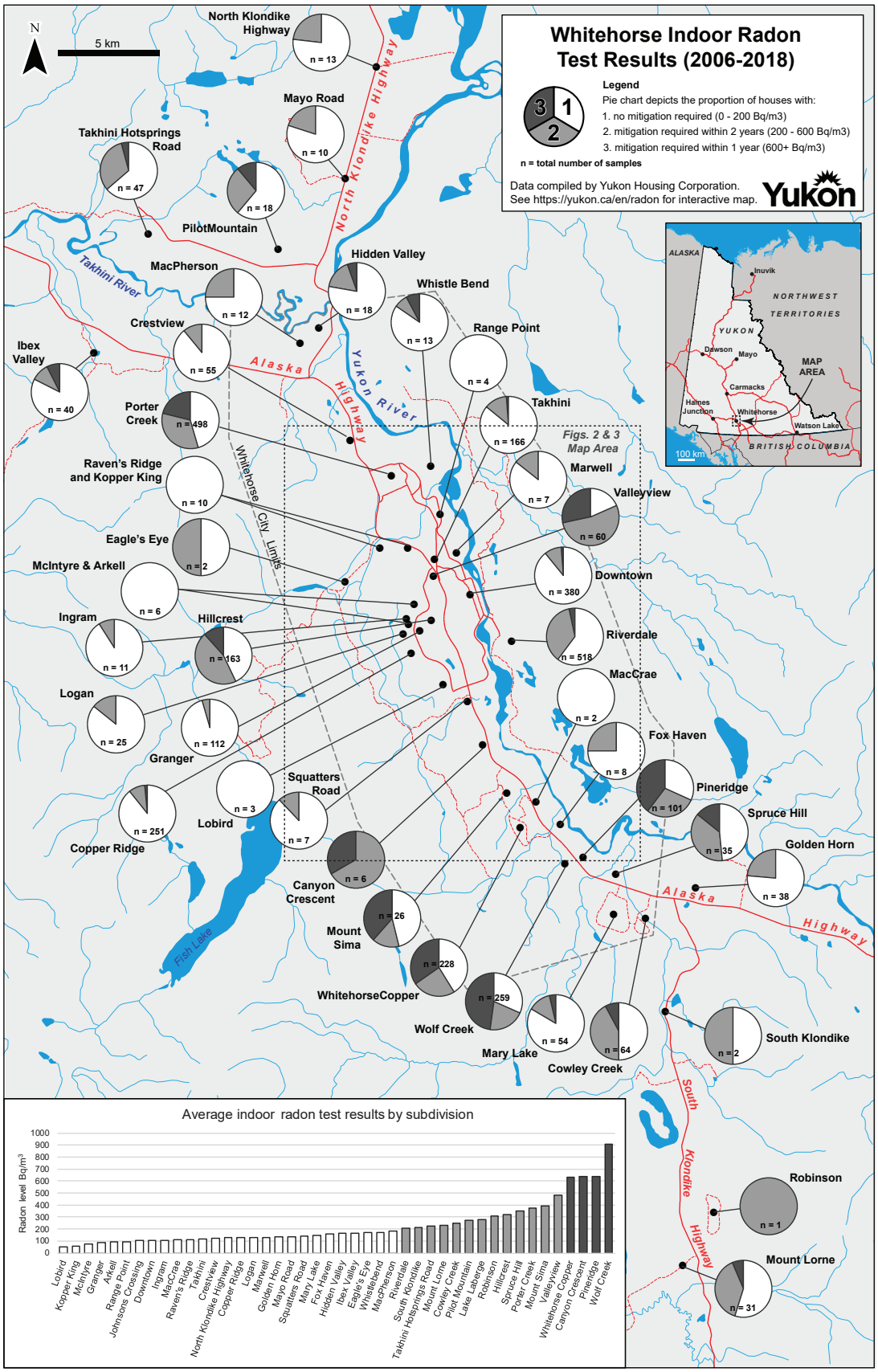

Figure 1. *Distribution and results of indoor radon tests compiled by Yukon Housing Corporation (Yukon Housing Corp., 2018). Sites in this study are located in Whistle Bend, Porter Creek, Raven's Ridge, Takhini, Granger, Copper Ridge, Riverdale, Squatters Road, Mount Sima, and Wolf Creek.*

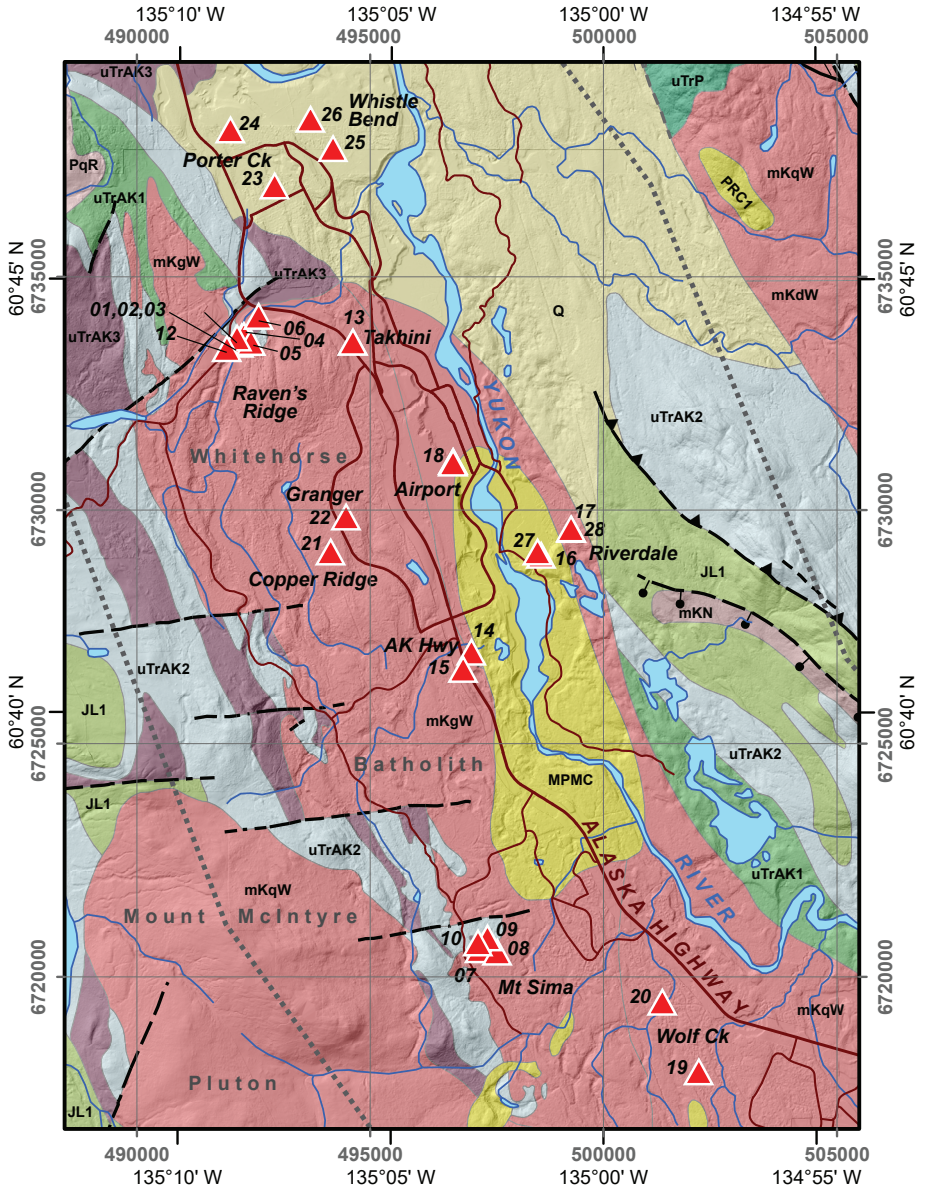

BEDROCK GEOLOGY (Yukon Geological Survey, 2020)

QUATERNARY
- Q: unconsolidated glacial deposits

MIOCENE TO PLIOCENE (LATE TERTIARY)
- MPMC: Miles Canyon basalt

PALEOCENE (EARLY TERTIARY)
- PRC1: Rhyolite Creek rhyolite and dacite
- PqR: Ruby Range Suite granite

MID-CRETACEOUS
- mKqW: Whitehorse Suite monzonite, granite and leucogranite
- mKgW: Whitehorse Suite granodiorite and diorite
- mKdW: Whitehorse Suite diorite
- mKN: Mount Nansen andesite to dacite

UPPER TRIASSIC
- uTrAK1: Casca shale, siltstone, sandstone, limestone
- uTrAK2: Hancock limestone
- uTrAK3: Mandanna sandstone, pebble conglomerate, mudstone
- uTrP: Povoas andesitic basalt flows, breccia, tuff, sandstone, argillite

LOWER AND MIDDLE JURASSIC
- JL1: Richtofen sandstone, siltstone, mudstone, conglomerate

Figure 2. *Bedrock geology of the Whitehorse area (Yukon Geological Survey, 2020a).*

from 2.4 to 5.2 ppm and thorium concentration varies from 10.2 to 16.2 ppm (Yukon Geological Survey, 2020b). During the Miocene and Pliocene, the Miles Canyon Basalt flowed northward from a vent near Mount Sima (Pearson *et al.*, 2001).

Surficial geology

The surficial geology of the Whitehorse area records a complex history of deposition by ice, water, and wind (Fig. 3). The McConnell Glaciation, which occurred from roughly 23.9 to 10.7 ka, was the most recent glaciation of the Whitehorse area (Bond, 2004). Ice flowed northward from the Coast Mountain and Cassiar lobes of the Cordilleran Ice Sheet and reached a glacial maximum by at least 18 ka BP. At this time, the Whitehorse valley was completely covered by ice. During deglaciation the ice underwent a fluctuating recession characterized by periods of stagnation and readvance. During periods of stagnation, several large glacial lakes formed in the Whitehorse area (Bond, 2004).

Five types of sediment were sampled in this study and classified according to their genetic origin (Bond *et al.*, 2005a–c): till, glaciofluvial sand and gravel, fine-grained glaciolacustrine sediment (sand, silt and clay), post-glacial fluvial sand and gravel, and eolian sand. Till deposits in the Whitehorse area are mostly lodgement tills, typically composed of a dense, unsorted matrix-supported diamicton deposited directly by ice, with most clasts derived from glacially-eroded bedrock, and a matrix that is predominantly sandy silt. Glaciofluvial gravels were deposited in terraces, kettled ice-contact complexes, and outwash channels as the ice receded, and typically comprise moderately sorted rounded pebbles and cobbles with a sandy matrix. A thick package of glaciolacustrine sand, silt and clay was deposited at the bottom of Glacial Lake Laberge. Dammed by ice to the south and a recessional moraine at the north end of Lake Laberge, this glacial lake occupied the Whitehorse area valley bottom during deglaciation (Brideau *et al.*, 2011). Shoreline deposits tend to be coarser and the lake sediments fine upward, reflecting the recession of the ice sheet and associated melt-water input. As Glacial Lake Laberge drained, the Yukon River delta migrated north with the shrinking shoreline, depositing a veneer of glaciofluvial sand on top of the lacustrine sediment. Winds reworked exposed riverbed sand and re-deposited it subaerially as dunes (Wolfe *et al.*, 2011). A veneer of fine-grained sandy silt loess, derived from deflation of the paraglacial surface, was also deposited over much of the study area. These deposits range from 10 to 50 cm thick. The Yukon River incised the thick glaciolacustrine deposits during the Holocene, forming sand and gravel terraces adjacent to the modern floodplain.

Radon

Sources of soil radon

Radon is a radioactive noble gas produced by the decay of radium, itself a decay product of uranium. Uranium occurs naturally, especially in granitic rocks, enriched veins, and ores such as pitchblende. Uranium-bearing rocks and minerals in surficial sediment provide a near-surface source for radon. The natural decay of uranium produces a steady supply of radon via diffusion through crystals and ejection from crystals by decay. Radon has a half-life of 3.8 days (Marin, 1956), and decays to the solid element polonium. Radon is mobile in both air and water, and can be transported to the surface through advection, dissolution in groundwater, diffusion, and passage through faults and fractured bedrock. At the surface, radon quickly dissipates in the atmosphere, and is therefore not hazardous in outdoor spaces.

Radon gas as a hazard

Radon is a recognized public health hazard (WHO 2009, Stanley *et al.* 2019) and is the second-leading cause of lung cancer in Canada. It is the leading cause of lung cancer among non-smokers, and the danger of radon lies in long-term exposure. The health risk is attributed to the radioactivity of ^{222}Rn and its radioactive daughters, which are inhaled and damage lung tissue when they decay. Health Canada recommends that remedial measures be taken to reduce radon in any dwelling to a concentration of 200 Bq m^{-3} or less (Government of Canada, 2020).

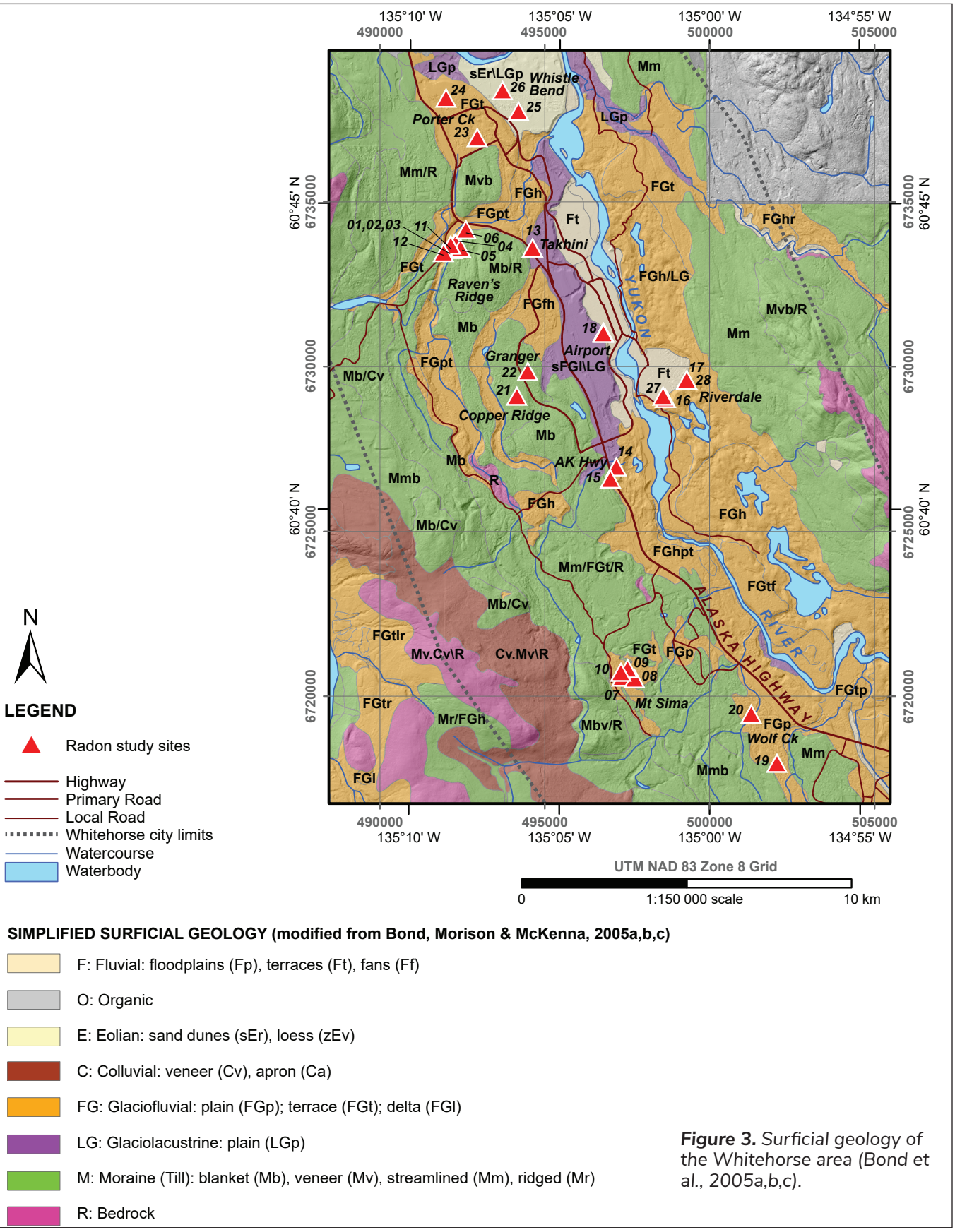

SIMPLIFIED SURFICIAL GEOLOGY (modified from Bond, Morison & McKenna, 2005a,b,c)

- F: Fluvial: floodplains (Fp), terraces (Ft), fans (Ff)
- O: Organic
- E: Eolian: sand dunes (sEr), loess (zEv)
- C: Colluvial: veneer (Cv), apron (Ca)
- FG: Glaciofluvial: plain (FGp); terrace (FGt); delta (FGl)
- LG: Glaciolacustrine: plain (LGp)
- M: Moraine (Till): blanket (Mb), veneer (Mv), streamlined (Mm), ridged (Mr)
- R: Bedrock

Figure 3. *Surficial geology of the Whitehorse area (Bond et al., 2005a,b,c).*

Previous radon studies in Yukon

The YGS undertook preliminary sampling of radon concentration in sediment at three control sites (20MK-013, 014, and 015) from fall 2019 to spring 2020. The present study incorporates these results. In addition to those soil radon measurements, Yukon Housing Corporation has compiled extensive indoor radon testing results from homes in Whitehorse and other Yukon communities for the 2006–2018 period (Fig. 1; Government of Yukon, 2020). Based on data compiled for the Whitehorse area, the highest concentrations of indoor radon occur in the Wolf Creek, Canyon Crescent, Pine Ridge and Whitehorse Copper subdivisions. Moderate indoor concentrations (still exceeding the Canadian guideline) are reported in several subdivisions, including Mount Sima, Porter Creek, and Riverdale. The Yukon government has also tested schools throughout Yukon and found that radon levels exceed the recommended level in three schools (Government of Yukon, 2018). In collaboration with the Yukon Lung Association and Yukon Housing Corporation, Angela Sabo has conducted indoor winter testing in neighborhoods with high concentrations and in First Nations housing; these data have not yet been published.

Field and analytical methods

Site selection

Sample sites were selected based on the presence of unambiguous uniform bedrock and surficial sediment type, known sediment thickness, and well-constrained surficial stratigraphy (from nearby water well or borehole logs). To achieve uniform bedrock controls, best attempts were made to cluster sample sites away from unit boundaries or known faults. Sites were chosen in representative, well-defined units so that results can be transferred to other areas in Yukon, and were placed in areas with little or no anthropogenic disturbance.

Sampling protocol

The Geological Survey of Canada protocol for measuring radon in soils (Friske *et al.*, 2010) was closely followed (Fig. 4). In particular, soil gas radon concentration was measured at five subsite locations within a 10 × 10 m area (Fig. 5) and revisited at least once, for a minimum of ten measurements per site during the summer season. Revisits were separated by at least one day. Radon results averaged for each site therefore provide an average concentration over both time and space. An example of a sampling site is provided in Figure 6.

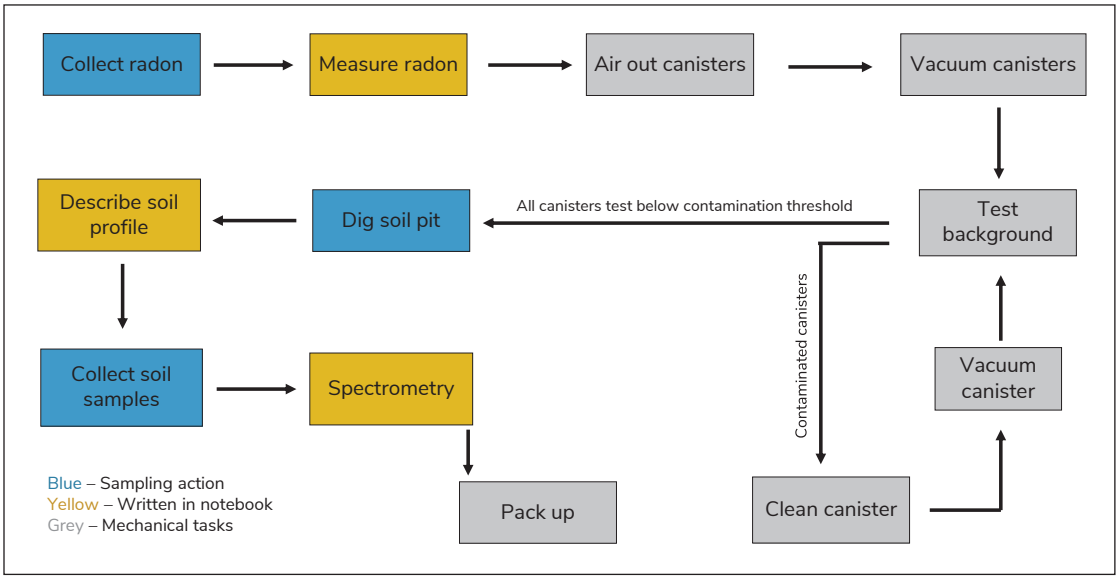

Figure 4. *Flowchart of sampling tasks during first visit to site. Based on protocol from Friske et al., 2010.*

The three control sites (20MK-013, 20MK-014, and 20MK-015) were sampled monthly for nine months and their data are incorporated into this study. Measured radon concentration in sediment, combined with clast lithology, geochemistry, grain size and soil moisture from each site, informed the analysis of suspected controls on radon concentration: bedrock composition, surficial sediment composition, depth to bedrock, surficial sediment grain size distribution, sediment maturity, and soil moisture.

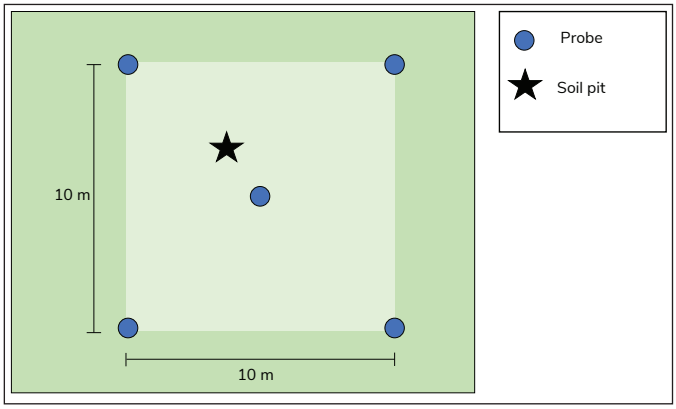

Figure 5. *Typical geometry of a sample site, with probes in corners and center of 10 × 10 m grid, and soil pit near the center probe. Exact placement of soil pit varied depending on position of trees, boulders, and other obstructions.*

Figure 6. *Photograph of sampling site 20MK-010 on June 18, 2020. Glaciofluvial gravel overlying Mandanna member of the Aksala Formation (sandstone and conglomerate). Three bags of sediment, from left to right, for clast lithology/geochemical analysis, matrix geochemistry, and grain size distribution. The spectrometer case is visible in top right and a probe flagged with orange tape can be seen in the top left.*

Radon collection

To ensure consistency with methodology used elsewhere in Canada, we followed the sampling protocols outlined by Friske et *al.* (2010), and used the same equipment and instruments described therein. Soil gas was collected from each site by inserting a piece of narrow metal pipe (hereafter referred to as a "probe") to a depth of 60 cm. A sharp steel point was placed at the groundward end of the probe, which was then hammered into the sediment with a mallet. A "punch rod," thinner and longer than the probe, was then tapped through the probe, pushing the tip roughly 5 cm deeper and creating an air cavity at the end of the probe. A 150 ml syringe was used to extract soil gas (Fig. 7). The first 150 ml of gas were purged to clear the probe of any atmospheric air, and the second volume was used to fill an evacuated ionization chamber (Fig. 8). Uncertainty in volume is estimated to be ± 10 ml (1σ). Concentrations were measured in situ using an ERM-3 Soil Radon Meter manufactured by Radon v.o.s. of Prague, using the protocol in the accompanying manual (included in Friske et *al.*, 2010). Some canisters did not fill completely, due either to low soil permeability and incomplete syringe fill, or to insufficient vacuum in the canister. In these cases the following error correction was applied according to the ERM-3 radon meter manual: $C_{cor} = C_{meas} \times \frac{150}{V_{in}}$, where C_{cor} is the corrected concentration measurement in kBq m^{-3}, C_{meas} is the concentration reported by the radon meter in kBq m^{-3}, and V_{in} is volume of soil gas extracted via syringe in ml.

Collection of other data

Additional geologic and environmental information relevant to radon concentration was also collected from each site. A >60 cm soil pit was hand dug and four sediment samples were collected from a depth of 60 cm (same depth as probe tips) for the following analysis: geochemistry of the matrix and representative clasts, sediment grain size, clast lithology on 50–100 pebbles, and soil moisture on 250 ml of sediment. If fewer than 50 clasts were available in the sediment, we collected as many as possible. The following sites had no clasts present: 20MK-006, 007, 11, 012, 013, 018, 025, 026 and 027. Gamma ray spectrometry was

conducted at each probe and soil pit to measure dose rate, potassium, equivalent uranium, and equivalent thorium. A wandering gamma ray survey of the site ensured that no areas produced anomalous levels of radioactivity (e.g., due to a granite boulder). The soil profile was described (horizon thickness, surficial sediment classification and evidence of disturbance), as well as local meteorological conditions (pressure, air temperature, humidity and wind), and a general description of the site was taken including topography and vegetation. Where accessible, bedrock samples for geochemical analyses were collected as close to the site location as possible.

Figure 7. *Soil gas extraction using 150 ml syringe. Red rubber tube connects directly to valve on ionization chamber. Probe flagged with orange tape.*

Figure 8. *IK-250 ionization chamber for radon concentration measurement, 250 ml capacity. Serial number is red, electrodes are brass pin at left and in central cylinder. Valve at right (knob above protruding tube).*

Analytical methods

Grain Size Distribution and Sorting

Approximately 1 kg of matrix sample was collected from each soil pit to determine grain size distribution. Clasts larger than 5 cm were removed by hand, as they are not considered part of the matrix. Grain size distribution was determined by Pacific Soil Analysis Inc. (Richmond, British Columbia) using sieve separation and a hydrometer. Two sets of sieve sizes were used: 3 inches, 19 mm, 8 mm, 4 mm, and 2 mm; and #10, #18, #35, #60, #140, 53 µm, and 2 µm. GRADISTAT Excel software (Blott and Pye, 2001) calculated sorting based on sieving data. This software returns arithmetic, geometric and logarithmic sorting statistics, as well as textural description based on the Folk and Ward classification. The sorting statistics reported here are all geometric.

Geochemistry

Approximately 0.5 kg of sediment matrix and representative pebble-sized clasts from each site pit were analyzed for major, minor, and other selected elements, and for loss on ignition. Whole rock geochemistry was completed at ALS Global (North Vancouver, British Columbia) using their complete characterization package. This included sample preparation and screening of the samples to 180 µm and the following analytical suite: whole rock by fusion/XRF, base metal by 4-acid digestion, loss on ignition for XRF, lithium borate fusion ICP-MS, and up to 34 elements by ICP-MS, as well as total carbon and total sulphur by IR spectroscopy. Results from the geochemical work are pending and therefore not presented in this paper.

Soil Moisture

Immediately before the radon gas measurement, soil moisture was determined by collecting a representative sample (roughly 0.5 kg of sediment) in a waterproof container from a depth of 60 cm in the soil pit. The sample was collected as soon as this depth was reached, to minimize evaporation upon exposure to the atmosphere. The sediment was weighed in the field (m_w) using a Starfrit High Precision Pocket Scale.

The same day, samples were baked at 100°C for one hour, cooled, and reweighed (m_d), and the difference in mass was used to estimate soil moisture (SM, %) according to $SM = \frac{m_w - m_d}{m_w} \times 100$.

Radon Gas Concentration

All measured data are reported, including any perceived anomalies. Mean radon concentration was calculated by first taking the average and standard deviation of all samples at a site, then removing measurements one standard deviation or greater from the mean (these are considered outliers) to determine if the standard deviation improved significantly, and finally recalculating mean and standard deviation of radon concentration with outliers removed. Weighted means were calculated according to the following formula: $W = \frac{\sum_{i=1}^{n} w_i x_i}{\sum_{i=1}^{n} w_i}$ where W is the weighted mean, x is a mean calculated by the above method, and $w = (1\text{-}COV).COV$ is the coefficient of variation (standard deviation divided by mean).

Results

Soil radon gas measurements

During the 2020 field season, 328 soil gas samples from 30 sites throughout the Whitehorse area were tested for radon concentration. Individual radon concentrations ranged from 0 to 68.1 kBq m^{-3}. Appendix 1 provides detailed characterization of each site based on field observations and borehole data. As shown in Figures 2 and 10, and in Appendix 1, the majority of sites (17 of 30) overlie granodiorite, while 6 overlie limestone, 3 overlie clastic sedimentary rocks, 2 overlie basalt, and 2 overlie unmapped bedrock. Depth to bedrock ranges from 1.5 m to greater than 100 m (the deepest being in Whistle Bend where glaciogenic sediments have not been drilled to bedrock). Twelve of the 30 sites are in glaciofluvial deposits, while 6 are in till, 5 are in fluvial sediments, 2 are in glaciolacustrine deposits, 1 is in eolian sediment, and 2 sample bedrock directly. Two sites are in sediment that was remobilized downhill from a till deposit onto a terrace, and are considered colluviated till. The grain size distribution of these samples is expected to be different from other till samples, but the clast lithology will be similar. Soil moisture varies from 2 to 14% by weight. Coefficients of variation range from 2 to 86%, with an average coefficient of variation of 27%. Variation is highest in silt and gravel units (average 62 and 29% respectively) and lowest in till and sand units (average 19 and 17%, respectively). The weighted means of each of the three major sediment types sampled in this study, weighted according to coefficient of variation, are 7.4 kBq m^{-3} for sand, 8.3 kBq m^{-3} for gravel and 16.0 kBq m^{-3} for till.

Seasonality

To determine if soil radon concentration varies seasonally, three sites (20MK-013, 20MK-014, and 20MK-015) were monitored monthly from August 2019 to August 2020, with a gap from February to April (Fig. 9). These were chosen as representative of sand, gravel, and diamict respectively. In diamict, the mean soil radon concentration is higher during the summer months, while in gravel the radon concentration is measurably lower in summer. Seasonal variation is less obvious in sand; however, December and January had the highest measured concentrations, suggesting a trend similar to that observed in gravel. Mean concentration is relatively consistent in all three sediment types during June, July and August.

Bedrock and surficial sediment type

We grouped mean radon concentration at each site according to the site's bedrock and surficial sediment type, and compared with depth to bedrock (Fig. 10). Within these groups, we calculated weighted means (according to coefficient of variation) for each bedrock and sediment type. No clear relationship between depth to bedrock and radon concentration is observed. The weighted means for sites overlying basalt and granodiorite are nearly identical (9.9 and 9.4 kBq m^{-3} respectively), and slightly higher for sites overlying limestone (13.5 kBq m^{-3}). Of the three parameters, the most influential control on radon concentration is surficial sediment texture. Diamicton has relatively high radon concentration, while sand is generally low and gravel is intermediate. The weighted mean for till is 16.0 kBq m^{-3}, while gravel and sand have similar weighted means with 8.3 kBq m^{-3} in gravel and 7.4 kBq m^{-3} in sand. There is a possible bimodality in gravel concentration, which may be related to sorting or to clast proportion.

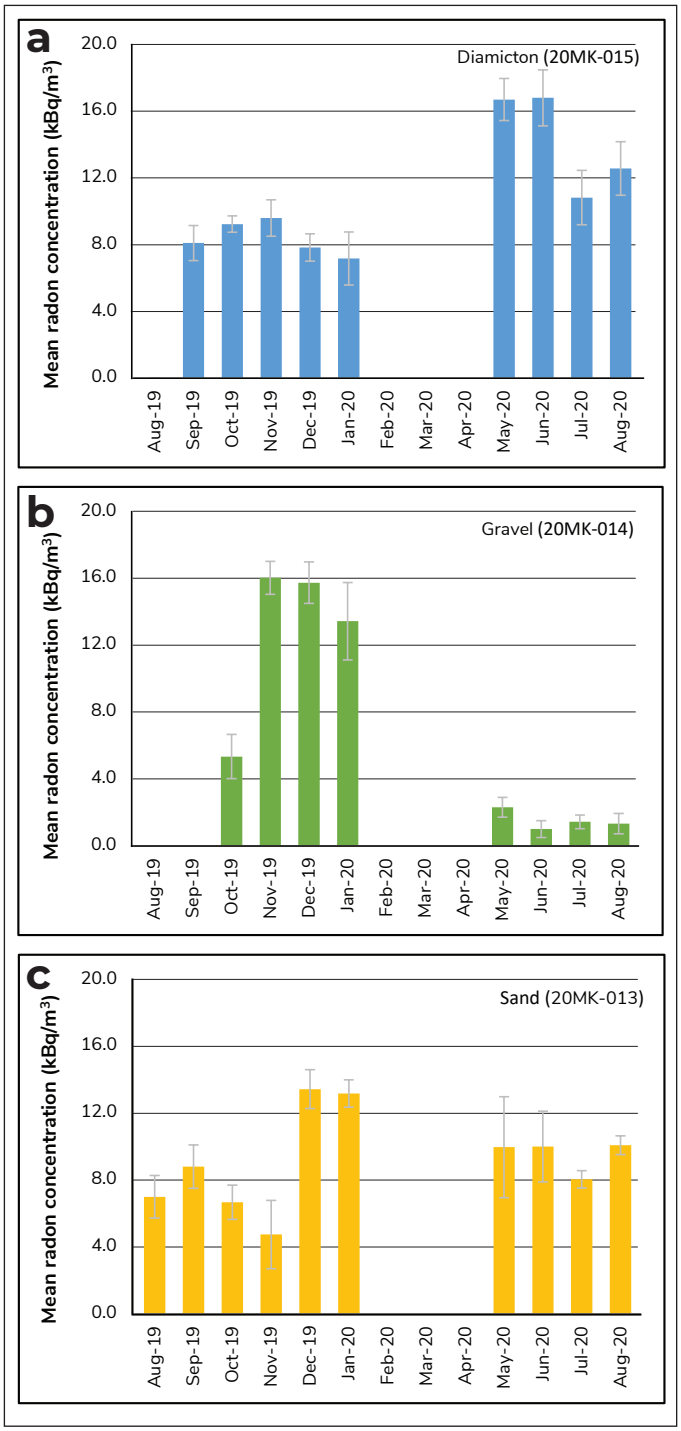

Figure 9. *Mean soil gas radon concentration at three long-term monitoring control sites. Data from* **(a)** *lodgement till,* **(b)** *glaciofluvial gravel, and* **(c)** *fluvial sand are plotted individually. Error bars are 1σ. Note that data are missing from February through April due to adverse winter sampling conditions and onset of global pandemic.*

Grain Size Distribution

In order to determine if there is a relationship between grain size distribution and radon concentration, we compared the mean radon concentration from each site to the fraction of matrix that is less than 53 µm in diameter (*i.e.*, silt and clay; Fig. 11). The tills (classified texturally as diamicton), along with reworked till that was reworked and deposited on a terrace, show the highest fraction of silt and clay in the matrix. The moderately sorted to very poorly sorted gravels consistently have relatively low abundances of fines, while sand displays a bimodal distribution of matrix grain size that is related to eolian versus fluvial/glaciofluvial origins. Results of the grain size analyses suggest a positive correlation between fraction of the matrix that is <53 µm diameter and radon concentration, with a coefficient of determination $R^2 = 0.59$.

Sorting

We also compared mean radon concentration at each site to the sorting of the matrix from the soil pit sample (Fig. 12). No obvious relationship was observed between radon concentration and matrix sorting. Since only the grain size distribution of matrix sample was analyzed, the sorting reported here does not reflect the overall sorting of the sediment. For example, till is typically more poorly sorted than gravel; however, some till samples had relatively well-sorted matrices. Descriptive classifications of the matrix, based on the schema of both Wentworth and Folk and Ward, are reported in Table 1. Although it does not represent the overall sorting of the sediment, matrix sorting may be used as a rough proxy for permeability, since uniform grain size increases permeability (see the section on Moisture).

Maturity

Maturity, or derivative degree of bedrock, may be a control on radon concentration. We therefore classified sediments, in order from least to most mature, as till, glaciofluvial sand and gravel, fluvial gravel and sand, glaciolacustrine silt, and eolian sand, then took a weighted mean for each sediment maturity level (weighted by the coefficient of variation), and compared these to radon concentration. Mean radon

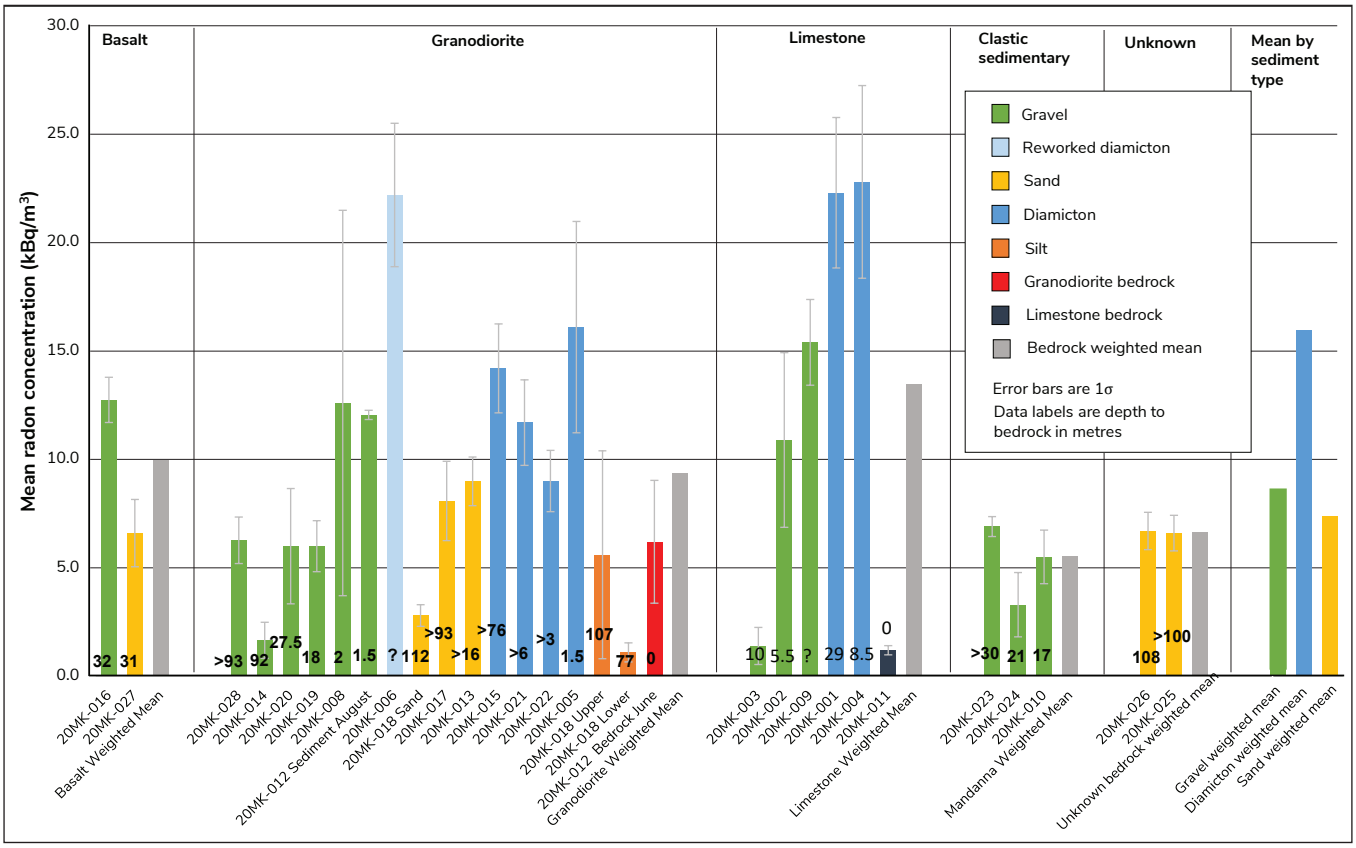

***Figure 10**. Mean soil gas radon concentration (min. 10 measurements) sorted by surficial material and bedrock characteristics. Concentration grouped by underlying bedrock type, and coloured according to overburden texture. Within each bedrock-surficial sediment class, concentrations are sorted by depth to bedrock (represented as data labels, in metres). Means weighted by coefficient of variation also calculated for each bedrock type (grey bars) and major surficial sediment texture (3 bars at far right).*

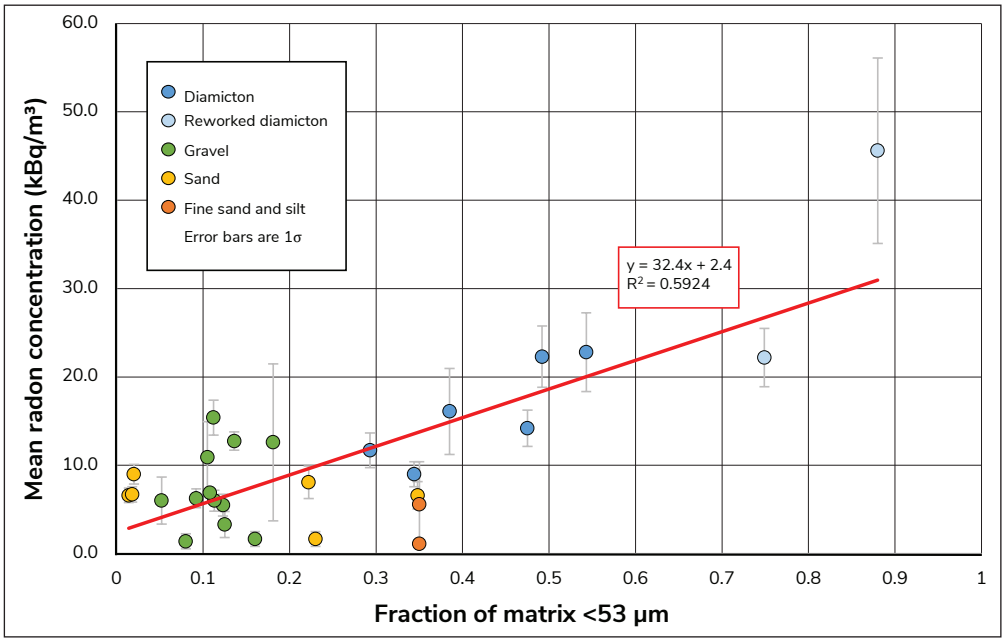

***Figure 11.** Mean radon concentration compared to the fraction of silt and clay in the sediment matrix. Data points are coloured according to surficial sediment type. Error bars are 1σ. Glaciolacustrine matrix samples were not collected so grain size distribution from Brideau et al. (2011) at a nearby sample location is used as a proxy for the two silt samples (orange).*

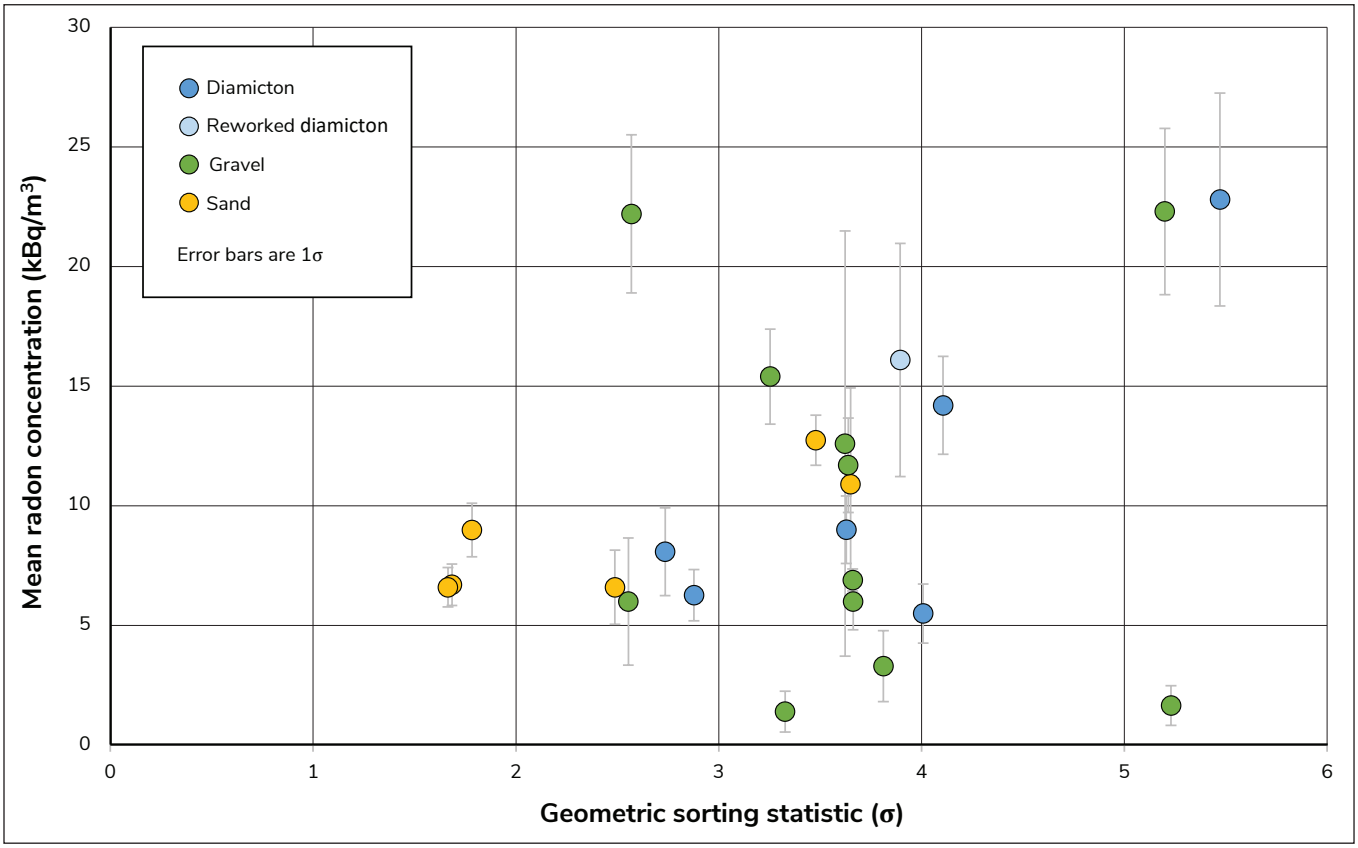

Figure 12. *Mean radon concentration compared to matrix sorting statistic as calculated by GRADISTAT Excel package (Blott and Pye, 2001). Greater values of geometric sorting statistic indicate poorer sorting of the matrix.*

concentration decreases with inferred sediment maturity, however not uniformly (Fig. 13). The coefficient of determination for linear best fit through the weighted means of each sediment type is $R^2 = 0.70$. This high coefficient of determination suggests that maturity is a strong negative control on radon concentration in sediment. It is a somewhat artificial measure; however, since the horizontal distribution of the groups is controlled only by the number of samples collected and is not directly related to the relative maturity of the sediment. Further work will include a more accurate estimation of maturity based on geochemistry.

Moisture

To determine the effect of sediment water content on radon concentration, we compared moisture measured in the soil pit with radon concentration from that site. A positive correlation between moisture and mean radon concentration is observed with a coefficient of determination $R^2 = 0.39$ (Fig. 14a). A positive overall trend also exists within each sediment type (Fig. 14b). Sand follows this trend the closest, with a coefficient of determination $R^2 = 0.99$; however, the dependence of concentration on moisture is also the lowest (shallowest slope). Gravel is the most scattered, and has the steepest trendline, with a coefficient of determination $R^2 = 0.29$ (Fig. 14b). Till has a coefficient of determination $R^2 = 0.44$. Sediment moisture depends on recent rainfall, and therefore sample timing; however, it may also illustrate the holding capacity of a sediment. Sediments with more silt and clay may hold more water than more permeable sands and gravels (see Fig. 15), and this may affect radon concentration. Note that the trendlines in Figure 14 do not take into account the uncertainties of each measurement, and are in some cases heavily affected by a single data point (e.g., rightmost point in Fig. 14a). The actual trends may therefore be less pronounced than those here represented.

Dominant controls

Of the controls compared in this study, maturity, moisture and silt/clay content of matrix appear to have the strongest correlations with mean radon concentration. Principal component analysis is required to determine properly which of these factors is the dominant control. For this preliminary study, we plotted moisture against silt and clay content to determine whether any correlation exists. We then compared these results to sediment maturity and radon concentration (Fig. 15). A positive correlation between moisture and matrix content is possible; however, a linear trendline has a relatively low coefficient of determination $R^2 = 0.19$. Radon concentration appears to increase both with increasing clay and silt content and with increasing moisture.

Table 1. *Description of matrix grain size, by textural group (based on Wentworth, 1922), geometric sorting statistic, and Folk and Ward (1957) classification. Note that grains 2–4 mm are considered "very fine gravel" by the Wentworth scale, and therefore several fine-grained sites (e.g., 20MK-006, 20MK-025 and 20MK-027) are described as "gravelly" in the second column.*

Site	Textural Group	Sigma (geo.)	Folk & Ward Mean	Folk & Ward Sorting
20MK-001	Gravelly Muddy Sand (diamicton)	5.2	Fine Sand	Very Poorly Sorted
20MK-002	Gravelly Sand	3.65	Very Coarse Sand	Poorly Sorted
20MK-003	Sandy Gravel	3.33	Very Coarse Sand	Poorly Sorted
20MK-004	Slightly Gravelly Muddy Sand (diamicton)	5.47	Very Fine Sand	Very Poorly Sorted
20MK-005	Gravelly Muddy Sand (diamicton)	3.89	Fine Sand	Poorly Sorted
20MK-006	Slightly Gravelly Muddy Sand	2.57	Very Fine Sand	Poorly Sorted
20MK-007	Slightly Gravelly Muddy Sand	2.14	Very Fine Sand	Moderately Sorted
20MK-008	Gravelly Sand	3.62	Medium Sand	Poorly Sorted
20MK-009	Gravelly Sand	3.25	Coarse Sand	Poorly Sorted
20MK-010	Sandy Gravel	4.01	Very Coarse Sand	Poorly Sorted
20MK-013	Sand	1.78	Medium Sand	Moderately Sorted
20MK-014	Gravelly Muddy Sand	5.23	Coarse Sand	Very Poorly Sorted
20MK-015	Slightly Gravelly Muddy Sand (diamicton)	4.11	Fine Sand	Very Poorly Sorted
20MK-016	Gravelly Sand	3.48	Medium Sand	Poorly Sorted
20MK-017	Slightly Gravelly Muddy Sand	2.74	Fine Sand	Poorly Sorted
20MK-019	Gravelly Sand	3.66	Very Coarse Sand	Poorly Sorted
20MK-020	Gravelly Sand	2.55	Coarse Sand	Poorly Sorted
20MK-021	Gravelly Muddy Sand (diamicton)	3.64	Medium Sand	Poorly Sorted
20MK-022	Gravelly Muddy Sand (diamicton)	3.63	Medium Sand	Poorly Sorted
20MK-023	Gravelly Sand	3.66	Very Coarse Sand	Poorly Sorted
20MK-024	Gravelly Sand	3.81	Coarse Sand	Poorly Sorted
20MK-025	Slightly Gravelly Sand	1.66	Coarse Sand	Moderately Well Sorted
20MK-026	Sand	1.68	Coarse Sand	Moderately Well Sorted
20MK-027	Slightly Gravelly Muddy Sand	2.49	Fine Sand	Poorly Sorted
20MK-028	Slightly Gravelly Sand	2.88	Coarse Sand	Poorly Sorted

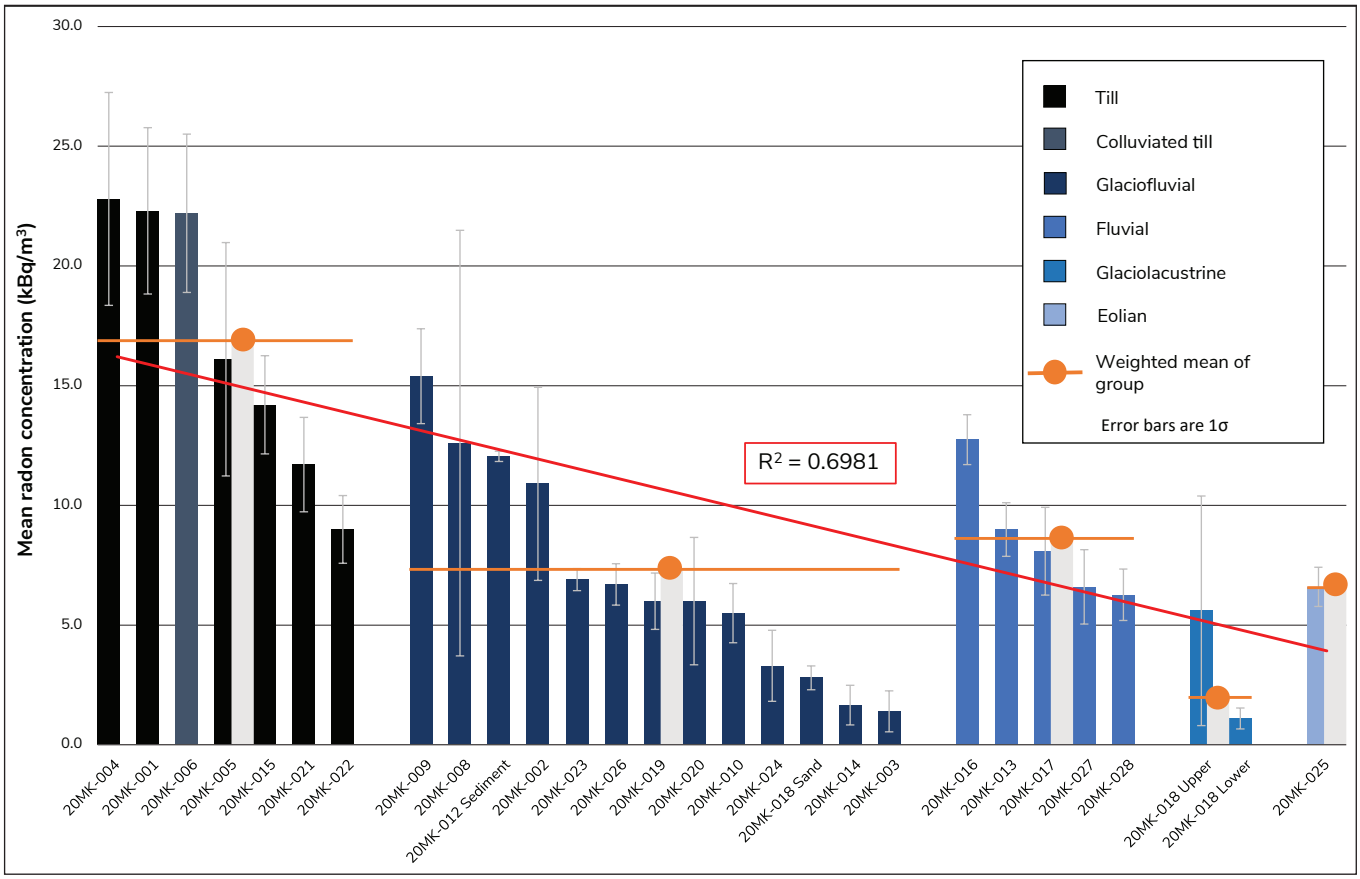

Figure 13. *Surficial sediment classified by maturity, or amount of modification from protolith. Since till is the most directly derived from bedrock, it is at the far left, followed by glaciofluvial, fluvial, glaciolacustrine, and eolian sediments. Note the colluviated till sample third from the left and that reworking (i.e., increase of maturity) has not had any appreciable effect on radon concentration. The average of each group is plotted as a flat line (orange), with a linear trendline in red. Not included in the graph to avoid skewing is 20MK-012, a grus site with mean radon concentration of 55 kBq m^{-3}. Since grus is more proximate to bedrock than till, this sample supports the overall trend of decreasing radon concentration with increasing maturity.*

Discussion and Implications

Seasonality appears to be an important non-geologic control on soil radon concentration in the region of Whitehorse, Yukon. While relatively consistent from May to August and from December to January, measured concentrations from 2019 and 2020 differ significantly between the two periods. Seasonal variability has been widely observed in outdoor and indoor studies (e.g., Siino et al., 2019, Yang et al., 2017, Barazza et al., 2015). However, not all sediment types in the Whitehorse region display consistent variation, as two sediment types exhibit higher and one sediment type lower radon concentrations in the summer (Fig. 9). A particular consideration for seasonal variation in Whitehorse is the seasonal freezing and thawing of ground, possibly creating a frozen cap which traps radon below the surface. Due to lower permeability in the silt-rich till (20MK-15), the retention of soil moisture as ice in the winter months may have reduced soil radon flux in the till more substantially.

The anti-phasing of the seasonal variation in radon concentration in different sediments motivated an analysis of the potential causes of non-seasonal variability in Yukon soil radon flux. Of the parameters evaluated—bedrock lithology, thickness of surficial cover, surficial sediment type, grain size distribution, sorting, sediment maturity, and soil moisture—silt and clay content of the matrix and sediment maturity appear to be the strongest geological controls on soil radon concentration in sediment.

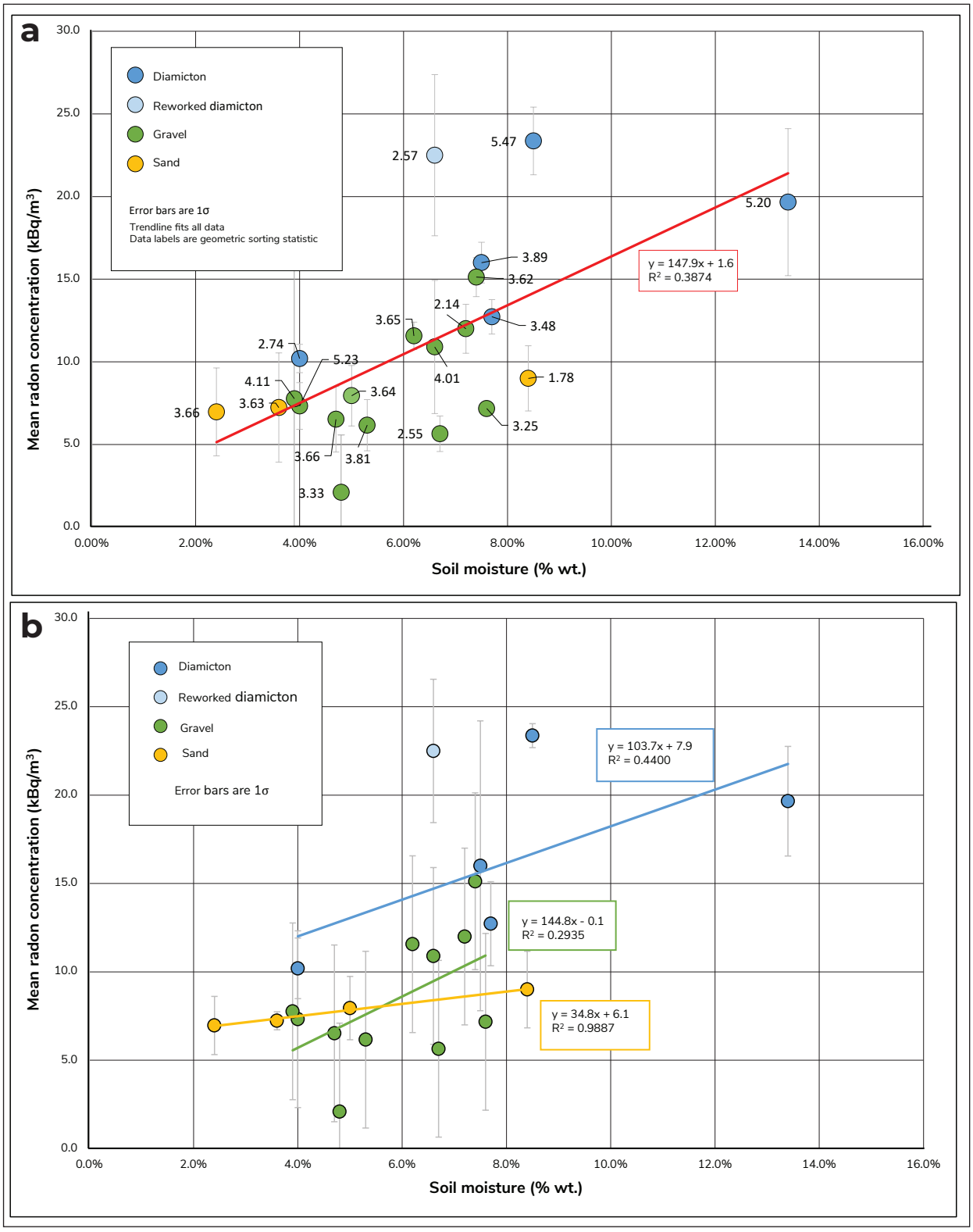

Figure 14. *Mean radon concentration compared to moisture at 60 cm depth. Trendlines calculated for* ***(a)*** *all samples and* ***(b)*** *each major sediment type. Data labels correspond to geometric sorting statistic of the matrix. Moisture is calculated as fraction of water by mass and was measured by mass difference of sediment from soil pit before and after heat treatment. All means were calculated only from measurements on the day a soil pit was dug (five measurements instead of ten).*

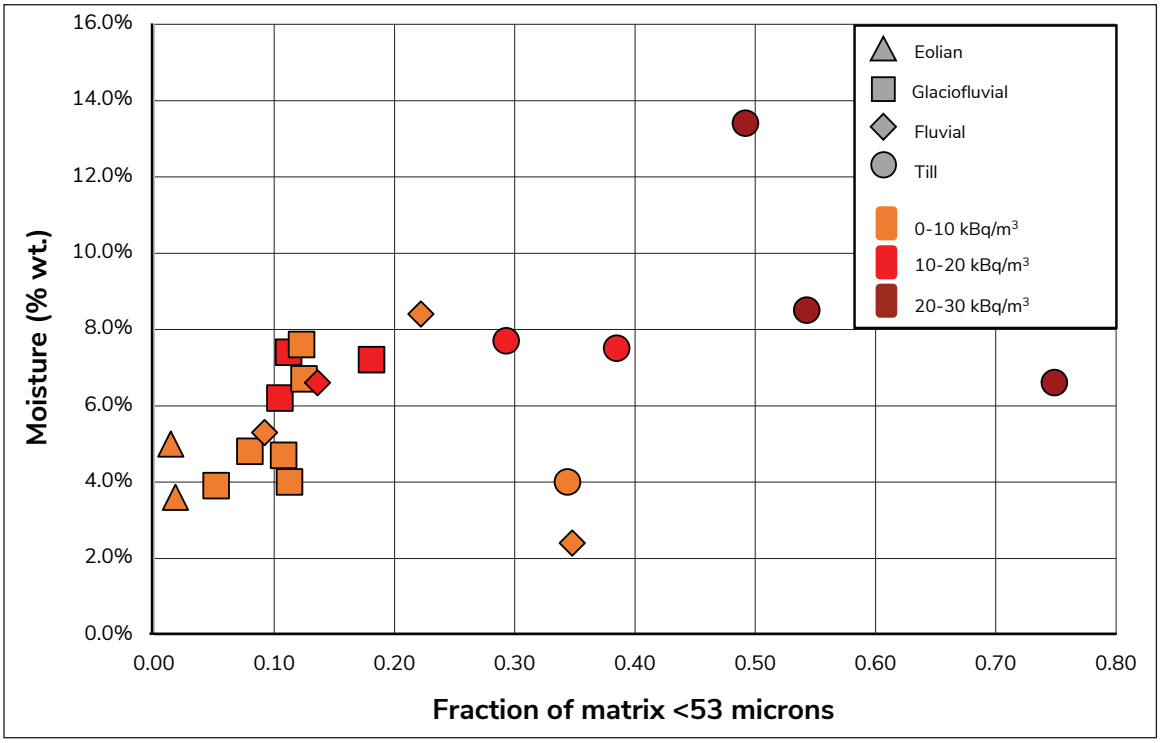

Figure 15. *Moisture at 60 cm depth compared to silt and clay content of matrix. Shapes correspond to genetic origin of sediment and colour corresponds to mean radon concentration. Trendline is not included due to low coefficient of determination.*

A grain size control in the study area is most evident from the positive correlation of radon concentration and quantity of silt and clay in the surficial sediment (Fig. 11). The observed seasonal anti-phasing seems to correspond with local differences in texture, where sites 20MK-013 and 20MK-014 have dominantly sandy matrices and overall textures of sand or gravelly muddy sand, whereas site 20MK-015 is a glacial diamicton with a greater silt component and therefore relatively lower permeability.

Grain size has previously been attributed as a first order control on radon flux (Saad *et al.*, 2018; Sakoda *et al.*, 2010; Markannen and Arvela, 1992). Fine-grained glaciolacustrine sediments examined in this study do not display high concentrations of radon however. This suggests that sediment maturity may also control radon concentration. For example, tills, which are relatively recently derived from bedrock and have sandy silt matrices, tend to contain high levels of radon compared to similarly fine-grained glaciolacustrine sediments. It is possible that as the glaciolacustrine sands and silts are reworked, the uranium-bearing minerals, *i.e.*, the radon sources, are weathered and destroyed. Overall, radon concentration tends to decrease with sediment maturity (Fig. 13).

A positive correlation is observed between radon concentration and moisture (Fig. 14), and this may reflect both average grain size and porosity of these sediments. Water may also facilitate the transport of radon by dissolution. To test the hypothesis that grain size and sediment maturity are the dominant controls of both spatial and temporal variability in soil radon, a principal component analysis should be conducted, and sediment mineral uranium concentrations need to be evaluated.

Depth to bedrock does not appear to be a first-order control on radon concentration, at least in areas where surficial material thickness is greater than 1 m (as is the case for the current study). A site in 1.5 m of sediment of overlying grus displays high concentrations of radon, suggesting that bedrock contributions may be important in areas of very shallow surficial cover.

In general, it seems that diffusion and emanation from bedrock minerals is not the sole source of radon nor is it a first-order control of spatial and temporal variability. Previous studies (e.g., O'Brien *et al.*, 2011) seem to support this observation, where bedrock-to-surface transport time exceeded the lifetime of ^{222}Rn. Variable isotopic composition of the different Quaternary sediment types overlying a single bedrock type could help further explain the source of variation in radon concentration.

In addition to our own and previous observations of the relationship between silt and clay content and soil radon concentration, it may be worthwhile to explore the escape of ^{222}Rn from uranium-bearing crystals. Emanation of ^{222}Rn is controlled by its recoil distance from the alpha decay of ^{226}Ra, which must therefore be within tens of micrometres of the grain surface for ejection to occur. The short half-life of ^{222}Rn and the low diffusivity at surface temperatures would suggest that diffusion of ^{222}Rn requires internal defects such as fission tracks that intersect with the grain surface. Therefore, sediments with finer grain sizes and higher surface area-to-volume ratio may have a larger contribution to soil gas radon, particularly if the fine fraction is a close derivative of bedrock. Furthermore, the fate of the ^{222}Rn after it escapes the grain may also be controlled by grain size, permeability, sorting, and moisture content. Sakoda *et al.* (2010) have considered some of these possible controls through numerical modeling, and their approach merits further analysis based on the available data from our study.

Almost all of the measured soil radon concentrations were above the Canadian recommended limit for indoor radon exposure of 0.2 kBq m^{-3}. An analysis of the link between soil radon concentration and indoor radon concentration is highly recommended in order to assess how surficial geology and architecture contribute to risks of radon exposure in Yukon.

In summary, our preliminary analysis of the 2020 soil radon data indicates that bedrock is not the single nor the most important source or control of near-surface soil radon concentration in the Whitehorse area. Of the surficial sediment parameters measured, silt and clay content of the soil matrix is the most closely correlated to radon concentration. Sediment maturity also appears to be a strong control on radon concentration, and this connection warrants geochemical analysis. Several meteorological factors, such as moisture and season, impart appreciable temporal variability on soil radon concentration among different sediment types. Future field programs targeting the source of variability should include more long-term continuous sampling at selected sites to evaluate the strength and reproducibility of the apparent seasonality, and additional sites in eolian and glaciolacustrine units are needed for a more representative characterization of the regional soil radon flux. We also recommend an overall increase in the number of sample sites to strengthen the statistics. Principal component analysis and investigation of ^{222}Rn diffusion will be completed once all geochemical data become available and will reported in a thesis by the lead author (Kishchuk, 2021).

Conclusions

Radon concentration was measured in sediment at 30 sites throughout the Whitehorse area. These sites represent till, glaciofluvial sand and gravel, fluvial sand and gravel, glaciolacustrine silt, and eolian sand. They overlie granodiorite, limestone, clastic sedimentary and basalt bedrock in various combinations. Almost all sites are in undisturbed sediment. A variety of geological controls (bedrock and sediment type, surficial cover thickness, grain size distribution, sorting, sediment maturity, soil moisture) and meteorological factors (rainfall, air pressure, wind, temperature) were compared to soil radon concentration. Conclusions reported here are preliminary as data collection and analysis are ongoing.

A notable seasonal shift in soil gas radon concentrations was observed at three long-term monitoring sites representing fluvial sand, glaciofluvial gravel and lodgement till. In the gravel site, radon concentration was at its lowest from May to August, while concentration in the diamict site was highest during these months. Relative to the seasonal variation, soil radon concentration was consistent during the summer months when most of this study was undertaken, and so intraseasonal variability likely had little effect on the results reported here.

Radon concentration is found to be independent of depth to bedrock, and shows no clear correlation with bedrock type. However, geochemical analyses of the sediments and bedrock are still pending, so a complete assessment of the importance of the underlying bedrock is not currently possible. Grain size distribution and sediment genesis appear to be the strongest geological controls on radon concentration in the surficial cover. It also appears that soil radon concentration correlates positively with soil moisture and negatively with sediment maturity.

Further analyses, including matrix geochemistry, clast lithology, and principal component analysis, will be undertaken next to confirm these results. Further work is also recommended to compare indoor radon concentration to radon concentration in sediment.

Acknowledgements

This project took place on the traditional territory of the Kwanlin Dün and Ta'an Kwäch'än First Nations. Thanks to Derek Cronmiller for reviewing this manuscript, and to staff at YGS this summer for their interest and input in this project. Brad Harvey (Geological Survey of Canada) kindly provided access to radon sampling equipment. YGS provided funding for the analyses and fieldwork. Funding to Michael Kishchuk was provided jointly by YGS and an NSERC Undergraduate Student Research Award at Dalhousie University. Special thanks to Paul Kishchuk and Kristina Craig of Whitehorse for providing a truck for fieldwork. Brett Elliot, of the YGS, produced Figure 1. Finally, we appreciate the generosity of landowners who let us sample on their property.

References

Barazza, F., Gfeller, W., Palacios, M. and Murith, C., 2015. An investigation of the potential causes for the seasonal and annual variations in indoor radon concentrations. Radiation Protection Dosimetry, vol. 167, p. 75–81.

Blott, S.J. and Pye, K., 2001. GRADISTAT: a grain size distribution and statistics package for the analysis of unconsolidated sediments. *Earth Surface Processes and Landforms*, vol. 26, p. 1237–1248.

Bond, J.D., 2004. Late Wisconsinan McConnell glaciation of the Whitehorse map area (105D), Yukon. In: Yukon Exploration and Geology 2003, D.S. Emond and L.L. Lewis (eds.), Yukon Geological Survey, p. 73–88.

Bond, J., Morison, S. and McKenna, K., 2005a. Surficial Geology of MacRae (NTS 105D/10), Yukon (scale 1:50 000). Yukon Geological Survey, Geoscience Map 2005-6.

Bond, J., Morison, S. and McKenna, K., 2005b. Surficial Geology of Whitehorse (NTS 105D/11), Yukon (scale 1:50 000). Yukon Geological Survey, Geoscience Map 2005-7.

Bond, J., Morison, S. and McKenna, K., 2005c. Surficial Geology of Upper Laberge (NTS 105D/14), Yukon (scale 1:50 000). Yukon Geological Survey, Geoscience Map 2005-8.

Brideau, M.-A., Stead, D., Bond, J.D, Lipovsky, P.S. and Ward, B.C., 2011. Preliminary stratigraphic and geotechnical investigations of the glaciolacustrine and loess deposits around the city of Whitehorse (NTS 105D/11), Yukon. *In:* Yukon Exploration and Geology 2010, K.E. MacFarlane, L.H. Weston, and C. Relf (eds.), Yukon Geological Survey, p. 33–53.

Cinelli, G., Tositti, L., Capaccioni, B., Brattich, E., and Mostacci, D., 2015. Soil gas radon assessment and development of a radon risk map in Bolsena, Central Italy. Environmental Geochemistry and Health, vol. 37, p. 305–319.

Colpron, M. (comp.), 2011. Geological compilation of Whitehorse trough – Whitehorse (105D), Lake Laberge (105E), and part of Carmacks (115I), Glenlyon (105L), Aishihik Lake (115H), Quiet Lake (105F) and Teslin (105C). Yukon Geological Survey, Geoscience Map 2011-1, 3 maps, scale 1:250 000, legend and appendices.

Folk, R.L. and Ward, W.C., 1957. Brazos River bar: a study in the significance of grain size parameters. Journal of Sedimentary Petrology, vol. 27, p. 3–26.

Friske, P.W.B., Kettles, I.M., McCurdy, M.W., McNeil, R.J. and Harvey, B.A., 2010. North American Soil Geochemical Landscapes Project: Canadian field protocols for collecting mineral soils and measuring soil gas radon and natural radioactivity. Geological Survey of Canada, Open File 6282, 177 p.

Government of Canada, 2020. Radon – What you need to know. Health Canada, https://www.canada.ca/en/health-canada/services/environmental-workplace-health/reports-publications/radon-what-you-need-to-know.html, [accessed December 10, 2020].

Government of Yukon, 2018. Radon testing in Yukon schools, https://yukon.ca/en/learn-about-radon-testing-yukon-schools#radon-testing-in-yukon-schools, [accessed November 30, 2020].

Government of Yukon, 2020. Radon Information, https://yukon.maps.arcgis.com/apps/MapSeries/index.html?appid, [accessed November 30, 2020].

Hart, C.J.R. and Radloff, J.K., 1990. Geology of Whitehorse, Alligator Lake, Fenwick Creek, Carcross and Part of Robinson Map Areas (105D/11, 6, 3, 2 and 7). Yukon Geological Survey, Open File 1990-4(G).

Kishchuk, M.J., 2021 (in prep.). Geological controls on radon concentration in surficial sediment in Whitehorse, Yukon. Unpublished honours thesis, Dalhousie University, Nova Scotia, Canada.

Marin, P.C., 1956. Measurement of the half-life of radon with a Curie-type ionization chamber. British Journal of Applied Physics, vol. 7, p. 188–190.

Markannen, M. and Arvela, H, 1992. Radon emanation from soils. Radiation Protection Dosimetry, vol. 45, p. 269–272.

O'Brien, K.E., Goodwin, T.A. and Risk, D., 2011. Radon soil gas in the Halifax Regional Municipality, Nova Scotia, Canada. Atlantic Geology, vol. 47, p. 112–124.

Pearson, F.K., Hart, C.J.R. and Power, M., 2001. Distribution of Miles Canyon basalt in the Whitehorse area and implications for groundwater resources. *In:* Yukon Exploration and Geology 2000, D.S. Emond and L.H. Weston (eds.), Exploration and Geological Sciences Division, Yukon Region, Indian and Northern Affairs Canada, p. 235–245.

Porstendorfer, J., 1994. Properties and behavior of radon and thoron and their decay products in the air. Journal of Aerosol Science, vol. 25, p. 219–263.

Saad, A.F., Abdallah, R.M. and Hussein, N.A., 2018. Physical and geometrical parameters controlling measurements of radon emanation and exhalation from soil. Applied Radiation and Isotopes, vol. 137, p. 273–279.

Sakoda, A., Ishimori, Y., Hanamoto, K., Kataoka, T., Kawabe, A. and Tamaoka, K., 2010. Experimental and modeling studies of grain size and moisture content effects on radon emanation. Radiation Measurements, vol. 45, p. 204–210.

Siino, M., Scudero, S., Cannelli, V., Piersanti, A. and D'Alessandro, A., 2019. Multiple seasonality in soil radon time series. Scientific Reports, vol. 9, 13 p.

Stanley, F. K. T., Irvine, J.L., Jacques, W.R., Salgia, S.R., Innes, D.G., Winquist, B.D., Torr, D., Brenner, D.R. and Goodarzi, A.A., 2019. Radon exposure is rising steadily within the modern North American residential environment, and is increasingly uniform across seasons. Scientific Reports, vol. 9, 17 p.

Wentworth, C. K., 1922. A Scale of Grade and Class Terms for Clastic Sediments. The Journal of Geology, vol. 30, p. 377-392.

West, K. and Donaldson, A., 2007. White River Ash, Yukon. Yukon Geological Survey, YGS Brochure 2007-1.

Wolfe, S., Bond, J. and Lamothe, M., 2011. Dune stabilization in central and southern Yukon in relation to early Holocene environmental change, northwestern North America. Quaternary Science Reviews, vol. 30, p. 324–334.

World Health Organization, 2009. WHO handbook on indoor radon: a public health perspective. WHO Press, Geneva, 94 p.

Yang, J., Buchsteiner, M., Salvamoser, J., Irlinger, J., Guo, Q. and Tschiersch, J., 2017. Radon exhalation from soil and its dependence on environmental parameters. Radiation Protection Dosimetry, vol. 177, p. 21–25.

Yukon Geological Survey, 2020a. Yukon digital bedrock geology. Yukon Geological Survey, http://data.geology.gov.yk.ca/Compilation/3#InfoTab, [accessed November 30, 2020].

Yukon Geological Survey, 2020b. Yukon Lithogeochemistry data set. Yukon Geological Survey, http://data.geology.gov.yk.ca/Compilation/35#InfoTab, [accessed December 1, 2020].

Yukon Housing Corporation, 2018. Whitehorse Indoor Radon Test Results 2006-2018. Yukon Housing Corporation, https://yukon.ca/en/radon, [accessed November 26, 2020].

Appendix 1 (digital only)

Sample site characteristics. Bedrock type, depth to bedrock, and soil pit profile are reported for each site, as well as elevation, geographic coordinates, vegetation type, estimates of drainage, and disturbance indicators. Drainage estimates are based on vegetation and underlying sediment type, while disturbance indicators are field observations such as tire-ruts, dug holes, and the presence of White River Ash in the soil pit. White River Ash was deposited roughly 1200 years ago following the eruption of Mt. Churchill in Alaska (West and Donaldson, 2007), and continuous tephra is taken to indicate an intact, undisturbed soil.